International Journal of Biological Macromolecules 273 (2024) 133079

Contents lists available at ScienceDirect

International Journal of Biological Macromolecules

journal homepage: www.elsevier.com/locate/ijbiomac

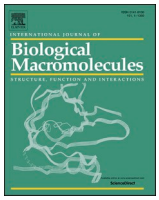

Effects of adding proteins from different sources during heat-moisture treatment on corn starch structure, physicochemical and *in vitro* digestibility

Xiuli Wu [*,1], Xuexu Wu [1], Jianwen Zhang, Xiangxuan Yan, Qing Zhang, Bingqian Zhang

College of Food Science and Engineering, Changchun University, Changchun, Jilin 130022, China

ARTICLE INFO

Keywords:
Different sources of protein
Protein-corn starch complexes
In vitro digestibility

ABSTRACT

Proteins impact starch digestion, but the specific mechanism under heat-moisture treatment remains unclear. This study examined how proteins from various sources—white kidney bean, soybean, casein, whey-altered corn starch's structure, physicochemical properties, and digestibility during heat-moisture treatment (HMT). HMT and protein addition could significantly reduce starch's digestibility. The kidney bean protein-starch complex under HMT had the highest resistant starch at 19.74 %. Most proteins effectively inhibit α-amylase, with kidney bean being the most significantly (IC_{50} = 1.712 ± 0.085 mg/mL). HMT makes starch obtain a more rigid structure, limits its swelling ability, and reduces paste viscosity and amylose leaching. At the same time, proteins also improve starch's short-range order, acting as a physical barrier to digestion. Rheological and low-field NMR analyses revealed that protein enhanced the complexes' shear stability and water-binding capacity. These findings enrich the understanding of how proteins from different sources affect starch digestion under HMT, aiding the creation of nutritious, hypoglycemic foods.

1. Introduction

Starch, as a primary storage carbohydrate, is a major energy source in the human diet, providing over 50 % of the body's energy requirements [1]. However, excessive intake of starch can lead to postprandial hyperglycemia, which, over time, may increase the risk of chronic metabolic diseases such as obesity, type II diabetes, and cardiovascular diseases. From a nutritional perspective, Englyst et al. [2] classified starch into three categories based on the rate of glucose release and absorption: rapidly digestible starch (RDS), slowly digestible starch (SDS), and resistant starch (RS). Reducing the content of RDS or increasing the levels of SDS and RS can effectively stabilize postprandial blood glucose levels, thereby reducing the risk of diabetes and related complications [3]. The digestion of starch is influenced by various factors, including the source of the starch, granule size, the ratio of amylose to amylopectin, structure, as well as other food components and processing conditions [4].

In practical diets, starch often coexists with non-starch components such as proteins and fats, and this complex mixture can significantly modulate the process of starch digestion [5]. Proteins, being the most abundant macromolecular organic substances in cereals aside from starch, whether endogenous or introduced during food processing, as well as their hydrolysis products such as peptides and amino acids, can modulate starch digestion. This regulation is primarily achieved by altering the morphological structure of starch or inhibiting the activity of digestive enzymes such as amylase. The mechanisms can be summarized as the formation of physical barriers, protein-starch interactions, and inhibition of α-amylase [6]. Currently, various exogenous proteins have been shown to slow down starch digestion [7,8]. Given the diversity of proteins, including differences in their structures (molecular weight, amino acid composition) and sources, the effects of different proteins on starch digestion vary [3]. Zhang et al. [9] found that rice proteins act as inert fillers, occupying the space within the starch matrix, thereby inhibiting starch swelling and molecular alignment, thus reducing the rate of starch digestion. In contrast, soy isolate proteins and whey isolate proteins can form network structures on the surface or within the starch matrix. These structures not only limit the swelling of starch but also act as physical barriers protecting

* Corresponding author at: No. 6543, Weixing Rd, Changchun University, Changchun, Jilin Province 130022, China.
E-mail addresses: wuxl@ccu.edu.cn (X. Wu), 220302127@mails.ccu.edu.cn (X. Wu), 220302133@mails.ccu.edu.cn (J. Zhang), 220301081@mails.ccu.edu.cn (X. Yan), 230301116@mails.ccu.edu.cn (Q. Zhang), 230301114@mails.ccu.edu.cn (B. Zhang).
[1] These authors contributed equally to this work.

https://doi.org/10.1016/j.ijbiomac.2024.133079
Received 18 March 2024; Received in revised form 22 May 2024; Accepted 9 June 2024
Available online 28 June 2024

starch from enzymatic degradation, thereby slowing down the rate of starch digestion. Studies have shown that hydrolyzed pea proteins more significantly reduce starch digestion compared to native pea proteins, while hydrolyzed soy proteins significantly reduce the RDS content in starch compared to native soy proteins [10]. The mechanisms by which different proteins inhibit α-amylase vary. Chen et al. [11] found that wheat gluten proteins inhibit α-amylase more strongly than soy isolate proteins. Wheat gluten proteins are mixed inhibitors of α-amylase, with both competitive and non-competitive inhibitory characteristics, while soy isolate proteins exhibit competitive inhibition. However, even proteins from the same source can have different mechanisms of amylase inhibition due to variations in protein content and differences among non-protein components [12].

Additionally, the digestibility of starch in starch-protein complexes can be influenced by numerous other factors, different processing methods that alter starch structure and thereby affect its digestibility [13]. Among various processing techniques, physical modification methods are favored in the food industry over biotechnology and chemical modifications because they avoid the introduction of potentially hazardous chemicals and genetically modified compounds [14]. Notably, heat-moisture treatment (HMT), a classic physical modification method, involves the thermal treatment of starch granules under specific moisture content (10–35 %) and strictly controlled temperatures (between the glass transition temperature and the pasting temperature) [15]. This method effectively adjusts the physicochemical properties of starch without destroying its basic granule structure, resulting in changes in starch crystallinity, granule swelling, and gelatinization behavior to meet specific food processing requirements. Due to the thermodynamic incompatibility between starch and proteins, pasting is commonly used to enhance the interaction forces between proteins and starch. This method not only disrupts the basic structure of starch granules but also limits starch's application in food processing. Some studies have demonstrated that HMT can maintain the basic structure of starch granules while enhancing the interactions between starch and proteins, thereby affecting starch digestion. Lu et al. [13] prepared rice starch-protein hydrolysate complexes through heat-moisture and annealing treatments, finding that these treatments significantly improved the thermal stability and resistance to digestion of the complexes. Similarly, research by Chen et al. [16] showed that starch-soy peptide complexes prepared using heat-moisture treatment exhibited superior resistance to digestion compared to those prepared by traditional physical mixing methods.

To explore the effects of different proteins under heat-moisture treatment (HMT) on the structure, physicochemical properties, and digestibility of starch, this study selected two plant proteins and two animal proteins. Soy protein isolate, whey protein, and casein, which are common high-quality protein sources, interact with starch through hydrogen bonding, electrostatic interactions, van der Waals forces, and hydrophobic interactions, influencing starch digestibility [6]. Currently, white kidney beans contain a unique glycoprotein called α-AI (α-amylase inhibitor), which has been proven to bind with α-amylase through non-competitive inhibition, altering the enzyme's molecular conformation and effectively preventing starch digestion [17]. However, research on the effects of white kidney bean protein on starch digestion is still limited. Our preliminary experiments suggest that white kidney bean protein has significant potential for improving starch digestion, making it a promising protein source for preventing obesity and diabetes. Therefore, the objectives of this study are: (1) to evaluate the impact of proteins from different sources on the structure, physicochemical properties, and digestibility of starch; (2) to investigate the effects of HMT on the interactions between different proteins and starch; and (3) to compare the effects of four proteins on starch digestion and verify the potential of white kidney bean protein in improving starch digestibility. These findings will provide a theoretical basis for further utilization and development of low-GI (glycemic index) foods containing white kidney bean protein and broaden the application of protein-starch complexes in food processing through HMT.

2. Materials and methods

2.1. Materials and reagents

White kidney bean was acquired from the local market. Soy protein isolate (SPI), containing 85.4 % protein, was sourced from Macklin Biochemical Technology Co., Ltd., Shanghai, China. Casein (CS) and whey protein isolate (WPI), with protein content of 86.3 % and 81.4 %, respectively, were obtained from Rhawn Reagent, Shanghai, China. Corn starch, comprising 23.42 % amylose, was procured from Jideli Food Co., Ltd., Suzhou, Jiangsu, China. Porcine pancreatic α-amylase, with an activity of 50 U/mg, was acquired from Sigma-Aldrich Co., St. Louis, MO, USA. Amyloglucosidase, exhibiting an activity of 100,000 U/mL, was purchased from Macklin Biochemical Technology Co., Ltd., Shanghai, China. All remaining chemicals used were of analytical grade.

2.2. Extraction of white kidney bean protein (KBP)

White kidney bean powder, subjected to peeling and sieving, was dispersed in deionized water at a 1:15 (*w/v*) solid-to-liquid ratio. Subsequently, the pH of the suspension was adjusted to 9.0 with 1 M NaOH. The mixture was continuously stirred for 2 h at room temperature, then centrifuged at 2583 ×*g* for 30 min. The resulting supernatant was collected and its pH was carefully brought down to the isoelectric point, ranging from 4.4 to 4.6, with 1 M HCl. This solution stood at 4 °C for 2 h to induce protein precipitation. After the resting period, the supernatant was decanted by centrifuging the mixture again at 2583 ×*g* for 30 min. The resulting protein-rich precipitate was thoroughly washed with deionized water, redissolved, and neutralized to pH 7. Finally, the protein solution was freeze-dried, ground, and sieved to yield the KBP.

2.3. Preparation of protein-starch complexes by heat-moisture treatment (HMT)

Protein-starch complexes were synthesized using a previously described method with the HMT process [16]. Initially, starch moisture content was adjusted to 30 % and allowed to equilibrate for 24 h at room temperature. Subsequently, protein was added at a 20 % (*w*/w) ratio relative to the dry starch weight and thoroughly blended. The mixture was sealed in an airtight container and heated at 100 °C for 12 h. Upon cooling, the mixture was dried at 45 °C overnight and sieved through a 100-mesh screen. The resulting samples with the addition of KBP, SPI, CS and WPI were denoted as HMT-KBP-S, HMT-SPI-S, HMT-CS-S, and HMT-WPI-S, respectively. A control sample of corn starch (S) treated with HMT alone, without protein addition, was labeled as HMT-S.

2.4. In vitro digestibility

The *in vitro* digestibility of the uncooked and cooked samples were assessed using a modified version of the Jia et al. method [18]. In brief, 200 mg of each sample (on a dry weight basis) was dispersed in 15 mL of sodium acetate buffer (pH 5.2, 0.2 M). To prevent starch aggregation, the cooked samples were stirred continuously in a boiling water bath for 30 min and then cooled to room temperature. Then, uncooked and cooked samples were incubated in a shaking water bath at 37 °C for 30 min. The digestion process commenced by introducing 10 mL of an enzymatic solution comprised of α-amylase (290 U/mL) and glucosidase (180 U/mL). Aliquots of 1 mL were withdrawn at predefined time points (0, 10, 20, 30, 60, 90, 120, 180, and 240 min). The enzymatic reaction was terminated promptly by adding 4 mL of absolute ethanol to each aliquot. The glucose released was quantified using the 3,5-dinitrosalicylic acid (DNS) method. The RDS, SDS, and RS contents were calculated using the following equation:

$$\mathrm{RDS}\ (\%) = \frac{0.9 \times (\rho_{20} - \rho_0) \times \mathrm{V}}{\mathrm{m}} \times 100 \quad (1)$$

$$\mathrm{SDS}\ (\%) = \frac{0.9 \times (\rho_{120} - \rho_{20}) \times \mathrm{V}}{\mathrm{m}} \times 100 \quad (2)$$

$$\mathrm{RS}\ (\%) = 100 - \mathrm{RDS}\ (\%) - \mathrm{SDS}\ (\%) \quad (3)$$

Where, ρ_0, ρ_{20} and ρ_{120} are the concentration of glucose (mg/mL) after digestion for 0, 20 and 120 min, respectively; V is the total volume of the reaction system (mL); m is the starch mass (g).

The *in vitro* digestibility curve of samples can be fitted to a first-order eq. [19]:

$$C_t = C_\infty \left(1 - e^{-kt}\right) \quad (4)$$

Where, C_∞ (mg/mL) is the glucose concentration at the end of the reaction; C_t (mg/mL) is the glucose concentration at time t; k (min^{-1}) is the reaction rate constant of starch samples.

2.5. Measurement of the α-amylase inhibitory activity

The inhibitory activity of α-amylase was determined using a method similar to that described by Sun et al. [20], with slight modifications. Briefly, 0.5 mL of porcine pancreatic α-amylase (4 U/mL) was mixed with 0.5 mL of protein solutions at different concentrations in a water bath at 37 °C for 10 min. Subsequently, 1 mL of gelatinized starch (1 mg/mL) was added, and the reaction was terminated by adding 5 mL of anhydrous ethanol after 10 min. After centrifugation at 2583 ×*g* for 20 min, 1 mL of the supernatant was mixed with 1 mL of DNS solution and heated in a boiling water bath for 5 min, followed by immediate cooling. The mixture was then diluted with 1 mL of deionized water, shaken well, and the OD value of the solution was measured at 510 nm using a multifunctional microplate reader (HBS-1096 A, Nanjing DeTie, Nanjing, China). During the measurement, blank, blank control, and suppression tubes were set up, and the volumes were filled with PBS (0.01 M, pH 7.2). The inhibition rate was calculated as follows:

$$\mathrm{Inhibitoryactivity}\ (\%) = \left(1 - \frac{\mathrm{A} - \mathrm{B}}{\mathrm{C} - \mathrm{D}}\right) \times 100 \quad (5)$$

Where, *A* is the sample reaction group (contains enzyme and protein); *B* is the sample blank group (contains protein but no enzyme); *C* is the control reaction group (contains enzyme but no protein) and *D* is the control blank group (contains neither enzyme nor protein). The half maximal inhibitory concentration (IC_{50}) of the four proteins were analyzed by combining SPSS regression after determining the respective OD values and plotting them according to concentration and inhibition.

2.6. Scanning electron microscopy (SEM) analysis

The samples were observed using a scanning electron microscope (JSM-6510LA, JEOL Ltd., Japan). Prior to observation, a trace sample was affixed to double-sided tape and sputter-coated with a thin layer of gold for observation. The particle morphology was observed with an accelerating voltage of 5.0 kV, with magnifications of 500 × and 1000 × .

2.7. Fourier transform infrared spectroscopy (FTIR)

FTIR analysis was performed using a Nicolet iS5 spectrometer (Thermo Fisher, USA). Approximately 1 mg of the sample was homogeneously mixed with 100 mg of KBr powder and pressed into a disc. The scanning parameters were set as follows: a spectral range from 4000 to 400 cm^{-1}, resolution at 4 cm^{-1}, with an accumulation of 16 scans [21]. Background spectra were acquired in the ambient air and subsequently deducted from the sample spectra. Prior to analysis, baseline correction and normalization were performed on each spectrum.

2.8. Pasting properties

The paste properties of the samples were determined using a Brabender viscometer (VISCOGRAPH-E, Duisburg, Brabender Technology Co. Ltd., Germany). The parameters were as follows: the initial temperature was set at 30 °C. Subsequently, the temperature was gradually increased at a rate of 5 °C/min until it reached 95 °C. At this temperature, the sample was maintained for 5 min. Afterward, the temperature gradually decreased to 50 °C at the same rate and held for 5 min. The pasting temperature (PT) and peak viscosity (PV), breakdown viscosity (BD), and setback viscosity (SB) were recorded.

2.9. Determination of amylose leaching content

The content of leached amylose in the samples was determined by referring to the method of Wu et al. [22] with minor modifications. 0.6 g of the sample was dispersed in 9.4 mL of deionized water and boiled in a water bath for 30 min. Cooled to room temperature and centrifuged at 8000 ×*g* for 20 min. From the resulting supernatant, a volume of 0.67 mL was carefully extracted and blended with 6 mL of 0.33 mol/L NaOH solution. This mixture was thoroughly homogenized, and a 0.1 mL aliquot of this solution was then added to 5 mL of a 0.5 % trichloroacetic acid (TCA) solution and 0.05 mL of a 0.01 mol/L I_2-KI indicator solution. The absorbance was measured against deionized water (used as a blank control) utilizing a UV–Visible spectrophotometer (UV-2700, Shimadzu Corporation, Japan) at a wavelength of 620 nm. The standard curve was constructed using an amylose standard, and the extent of amylose leaching in the supernatant was calculated ($y = 0.0069x\text{-}0.0730$, $R^2 = 0.9991$).

2.10. Swelling power

The SP of the samples was evaluated using Hu's method [23]. Briefly, 1 g of the sample was dispersed in 25 mL of deionized water. This suspension was then subjected to a controlled thermal treatment within a water bath at 75 °C, 85 °C and 95 °C for 30 min. The dispersion was vortex-shaken every 10 min. Subsequent to the heat treatment, the samples were quickly cooled in an ice bath and then centrifuged at 3000 ×*g* for 20 min. The following equation was used to calculate the SP:

$$\mathrm{SP}\ (\mathrm{g/g}) = \mathrm{M_P}/\mathrm{M_d} \quad (6)$$

Where, M_p (g) is the weight of sediment and M_d (g) is the weight of sediment after drying at 105 °C.

2.11. Rheology measurement

2.11.1. Steady shear rheological properties

A 6 % (*w*/w) sample suspension was heated to 95 °C and maintained at this temperature for 30 min. Following this, the resulting starch paste was cooled to room temperature and transferred to a rheometer (RHEOMETER RS3, Brookfield, USA) for further analysis.

During the rheological measurements, the shear rate applied to the samples was varied within the range of 0.1 to 300 s^{-1} and then reversed from 300 to 0.1 s^{-1}, all while maintaining a constant temperature of 25 °C. The collected data points were subsequently analyzed using the Ostwald-de-Waele eq. [24].

$$\tau = K \times \dot{\gamma}^n \quad (7)$$

Where, $\dot{\gamma}$ (s^{-1}) is shear rate, τ (Pa) is shear stress, n is fluid index and K (Pa s^n) is consistency coefficient.

2.11.2. Dynamic rheological properties

The dynamic rheological properties of the samples were measured using a rotational rheometer (RSO, Brookfield, USA). The method was based on that described by Lu et al. [13] with slight modifications. A 6 %

starch suspension (*w*/w) was gelatinized in a boiling water bath for 30 min. After cooling, the samples underwent dynamic rheological testing within a frequency range of 0.1–10 Hz. The strain amplitude was set at 3 % within the linear viscoelastic region. The dynamic rheological results encompassed the storage modulus (elastic characteristic parameter G', Pa), loss modulus (viscous characteristic parameter G", Pa), and loss factor (tan δ = G"/G').

2.12. Low-field nuclear magnetic resonance (LF-NMR)

The water mobility in S, HMT-S, and protein-starch complexes were analyzed by a LF-NMR analyzer (MesoMR23–060 *V*-I, Niumag Co. Ltd., Suzhou, China) [9]. A 6 %(*w*/w) starch suspension was heated in boiling water bath for 30 min to obtain sample gel. After gelation, the sample gels were transferred into glass vials and equilibrated at 25 °C for 30 min. The samples were placed into an NMR tube for the measurement, and the Q-CPMG sequence was selected for the test. The echo time was set to 0.1 ms, with 15,000 echoes and 16 accumulations performed. The inversion images are analyzed using instrumental software.

2.13. Statistical analysis

All experiments were conducted in triplicate, and data were expressed as mean ± standard deviation. Analysis of variance (ANOVA) and Tukey's HSD test were carried out using SPSS version 26.0 (SPSS Inc., Chicago, USA). Differences in means and F-tests were considered significant when $P < 0.05$.

3. Results and discussion

3.1. In vitro starch digestibility

The effect of protein on starch digestion can be divided into "physical" and "chemical" effects. The dominant effect of protein on starch digestion is different in uncooked and cooked starch samples [25]. The HMT used in this study can maintain the basic structure of starch granules, so the digestion of uncooked samples was studied. In addition, most starch and starch-based foods that people eat undergo various types of processing or cooking. To enhance relevance to practical applications, the digestion of cooked (pasted) samples was also measured. The results are shown in Fig. 1.

3.1.1. Uncooked samples

The enzymatic hydrolysis kinetics curve and RDS, SDS and RS contents of uncooked samples are shown in Fig. 1(a) and (b). Compared with S, HMT-S after HMT had higher C_∞ (87.71 ± 1.44 mg/mL) and RDS content (29.79 ± 0.38 %). This is because HMT promotes the crystal destruction and dissociation of the double helix structure of starch granules, increases the opportunity for enzymes to contact starch molecules, and facilitates enzymatic hydrolysis in granules [16]. Adding KBP, SPI, CS and WPI during HMT significantly decreased C_∞ and RDS contents of starch. The C_∞ of HMT-KBP-S, HMT-SPI-S, HMT-CS-S and HMT-WPI-S were 22.55 ± 0.61 mg/mL, 25.10 ± 0.59 mg/mL, 28.14 ± 1.39 mg/mL and 25.87 ± 1.88 mg/mL, respectively. RDS content were 7.88 ± 0.10 %, 10.94 ± 0.60 %, 8.57 ± 0.17 % and 7.29 ± 0.20 % respectively. It indicates that adding exogenous proteins during HMT can significantly reduce starch digestibility. The effects of water, heat and pressure during HMT may enhance protein-starch interactions [16], thereby reducing starch digestibility. In addition, heat-induced structural changes in protein components lead to cross-linking of proteins, which to some extent protects starch from amylase damage [26].

3.1.2. Cooked samples

The enzymatic hydrolysis kinetics curve and RDS, SDS and RS contents of cooked samples are shown in Fig. 1(c) and (d). Compared with uncooked samples, the starch hydrolysis rate in cooked samples increased significantly. During the cooking process, starch particles swell due to water absorption, and the ordered crystal structure of

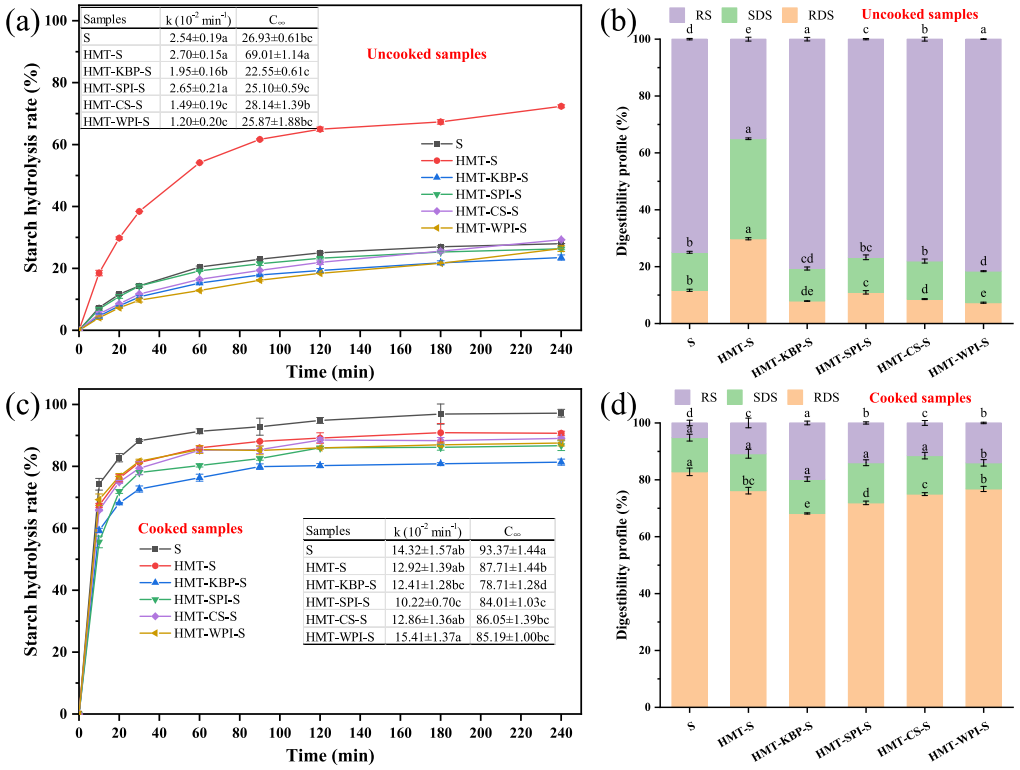

Fig. 1. Kinetic curves of the enzymatic hydrolysis rates of (a) uncooked samples and (c) cooked samples. The RDS, SDS and RS content of (b) uncooked samples and (d) cooked samples. Data are presented as means ± standard deviations. Different lowercase letters indicated a significant difference in the same color ($P < 0.05$).

molecules is destroyed under hydrothermal action, which increases the opportunity for enzymes to contact starch molecules. Thus, the hydrolysis rate of cooked samples increases significantly. In contrast with undercooked HMT-S, cooked HMT-S has a lower digestibility than S. Wang et al. [27] suggested that HMT reduces starch digestibility by converting part of RDS to SDS and RS. At the same time, HMT changed the structure of starch granules, making starch granules harder, limiting starch gelatinization and expansion [28]. This alteration also reduced the sites combined with enzymes, and reducing digestibility. Consistent with uncooked samples, exogenous protein could alleviate starch digestibility. Protein reduces starch digestibility for many reasons. As proteins contain many hydrophilic groups, they are linked to starch by hydrogen bonds, inhibiting the hydrolysis of starch by enzymes [29,30]. Also, proteins can affect starch digestibility by inhibiting amylase activity. However, in cooked starch samples, the *in vitro* digestibility of starch was more affected by the physical barrier of the protein than by chemical effects [3,25]. HMT-KBP-S had the lowest digestibility among the four complexes, which may be related to the looser structure of KBP (more β-turns and random coil structures, Table S1).

3.2. Measurement of the α-amylase inhibitory activity

Inhibiting amylase activity is one of the effective ways to slow down starch digestibility. Some studies have shown that some proteins have an apparent inhibitory effect on α-amylase [31]. In this study, the content of reducing sugar in starch hydrolyzed by α-amylase was determined by adding different protein concentrations to explore the inhibitory effect of protein on α-amylase activity. As shown in Fig. S1, the addition of KBP, SPI and WPI reduced the reducing sugar production rate. The inhibitory effect of different proteins on α-amylase varied, but they all showed concentration dependence. However, the inhibitory effect on α-amylase activity decreased when the protein concentration reached a certain level. This may be due to saturation of the binding site where the protein interacts with α-amylase [32]. From the half maximal inhibitory concentration (IC_{50}) given in Fig. S1, it can be seen that KBP (IC_{50} = 1.712 ± 0.085 mg/mL) had a strong α-amylase inhibitory effect,

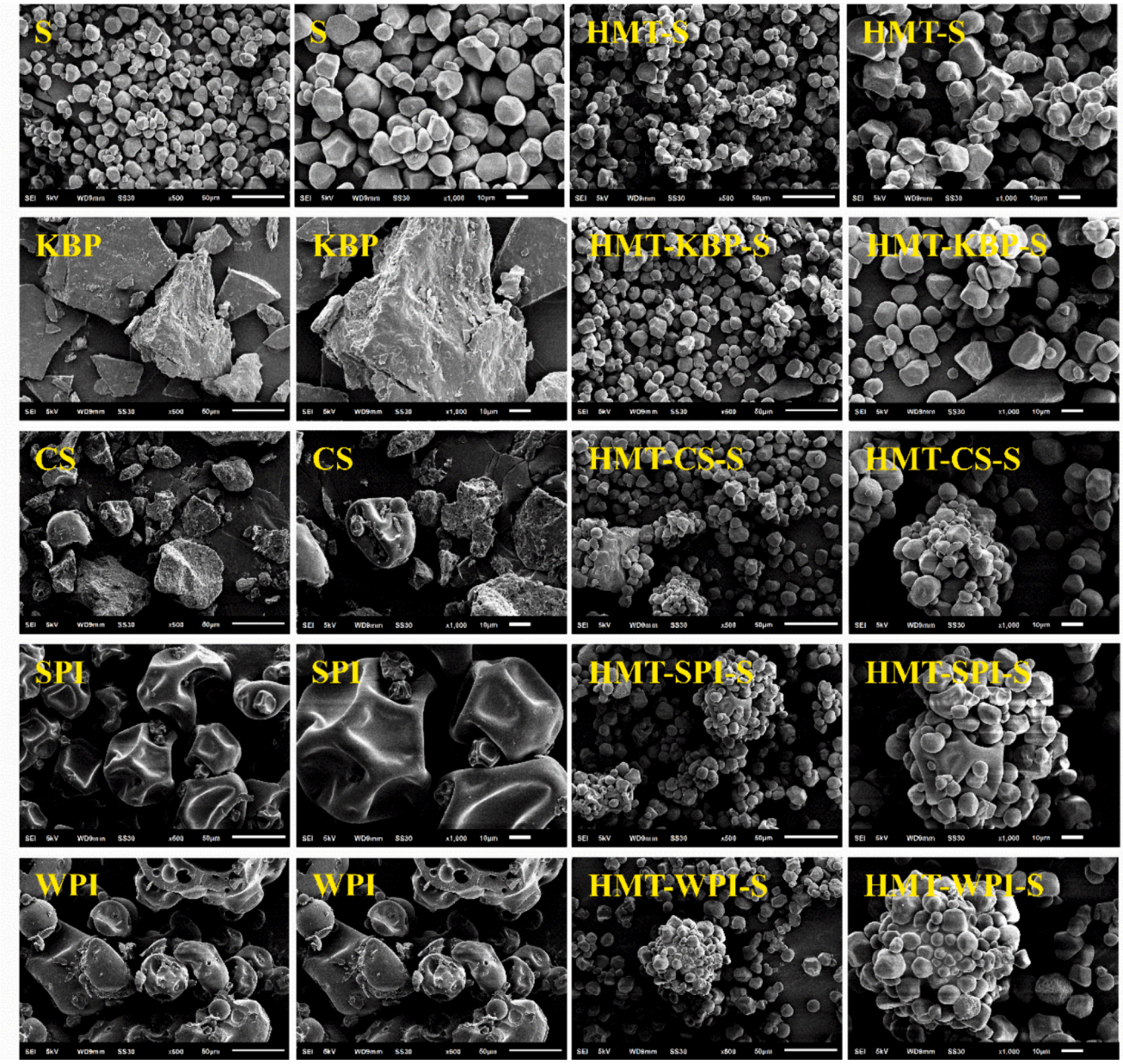

Fig. 2. Scanning electron microscopy of the samples (same sample with a magnification of 500× observed in the left image and 1000× observed in the right image).

followed by SPI (IC_{50} = 1.949 ± 0.107 mg/mL), and lastly, the WPI (IC_{50} = 2.083 ± 0.146 mg/mL). It is noteworthy that CS did not exhibit an inhibitory effect on α-amylase.

Out of the four proteins, KBP had the greatest inhibitory impact on α-amylase, as evidenced by the IC_{50} values and the curves representing the inhibition rate of α-amylase in Fig. S1. Wang et al. [32] in their study of red kidney bean protein, also found that red kidney bean protein inhibited α-amylase in a non-competitive manner and that its inhibition was concentration-dependent. In contrast, SPI and WPI showed weaker inhibitory effects, possibly related to their protein types, amino acid compositions, spatial structures and surface groups. The reason why CS did not show an inhibitory effect on α-amylase in the experiment may be related to the fact that CS is more difficult to dissolve in water and the exposed hydrophobic groups of its molecule, which leads to the difficulty of effective binding with the active site of α-amylase, thus making its inhibitory effect on α-amylase weaker. The results of subsequent SP experiments support this view.

3.3. SEM

Fig. 2 illustrates the microstructure of the samples. Natural corn starch is polyhedral or spherical with a smooth surface. After HMT, HMT-S aggregated, and the particle surface became rougher; some particle surfaces appeared depressed or even collapsed. This phenomenon is consistent with that observed by Wang et al. [27], where some particles gel at high moisture content (30 %) HMT, resulting in inconsistent swelling of particles and the appearance of surface pits. Due to the limitation of moisture content, HMT can cause partial starch gelatinization, which mainly exists on the surface of starch granules, and the increase in surface viscosity leads to granule aggregation. During the subsequent cooling process of HMT, gelatinized starch molecules (mainly amylose molecules) will re-form a denser structure through hydrogen bonds, making it difficult for digestive enzymes to contact and decompose starch, so HMT-S has a lower digestibility than S.

The four proteins were large; KBP showed a large lamellar structure, and CS, SPI, and WPI showed a spherical structure. In these four complexes, the aggregation phenomenon in HMT-KBP-S is not apparent; most KBPs disappear, and only a few small KBPs exist. This may be due to the looser structure of KBP (more β-turn and random coil, Table S1), which is better compatible with starch during HMT, coating the starch granule surface. The other three complexes are starch attached to the surface of protein granules, and some starch granules are aggregated. This results in the physical barrier effect of proteins in these three complexes being weaker than that of KBP in the HMT-KBP-S complex. HMT-KBP-S has a solid physical barrier effect and thus has low digestibility in all samples, which is consistent with the digestibility results.

3.4. FTIR

Fig. 3(a) shows FTIR spectra of samples. No new characteristic peaks were found for all HMT complexes, suggesting no covalent interactions between S and the protein occurred during HMT. The band around 3200–3600 cm^{-1} is attributed to -OH stretching [33]. With the addition of four proteins, the peak shifted to lower wavenumbers (HMT-KBP-S, HMT-SPI-S, HMT-CS-S and HMT-WPI-S shifted from 3439.9 cm^{-1} to 3415.8 cm^{-1}, 3381.1 cm^{-1}, 3419.7 cm^{-1} and 3385.4 cm^{-1}, respectively), indicating the enhancement of hydrogen bonding between starch and protein. This may be due to hydrogen bonds that can form between the -OH groups and polar residue side chains in starch and between amino and carbonyl groups in protein [34]. The peak shift of different proteins is different. This indicates that the degree of protein binding to the starch matrix through hydrogen bonds differs. Protein binding to starch is enhanced, as is the ability to inhibit starch digestibility. The typical bands at 1580–1720 cm^{-1} and 1480–1580 cm^{-1} belong to amide I and amide II of the protein [35].

The effect of protein on the short-range ordered structure of starch was analyzed by deconvolution of 800–1200 cm^{-1} band. 1047 cm^{-1} and 1022 cm^{-1} are related to crystalline structure and amorphous structure of starch respectively. 995 cm^{-1} represents hydrogen bonds formed between hydroxyl groups of starch molecules. By calculating R_1 (1047/1022 cm^{-1}) and R_2 (1022/995 cm^{-1}) (Table 1), the short-range ordered structure and hydrogen bond strength of starch were expressed [36]. After HMT, R_1 of HMT-S decreased, indicating that HMT can destroy the starch structure. Under HMT condition, the R_1 value of starch complex was increased after adding protein, which indicated that adding protein could improve the ordering degree of starch. The increase of R_2 also indicates the increase of hydrogen bond strength of starch molecule [37]. The increase in order and hydrogen bond strength means the structure is not easily degraded by amylase and digested.

3.5. Pasting properties

Fig. 4(a) and Table 1 show pasting curves and pasting characteristics of corn starch and its complexes with different proteins under HMT, respectively. The pasting curves of starch-water suspensions as a function of time and temperature are commonly used to determine pasting characteristics, including PT, PV, BD and SB. Phase changes involved in starch pasting associated with water diffusion into granules, exudation of macromolecules, disruption of ordered structures, disappearance of

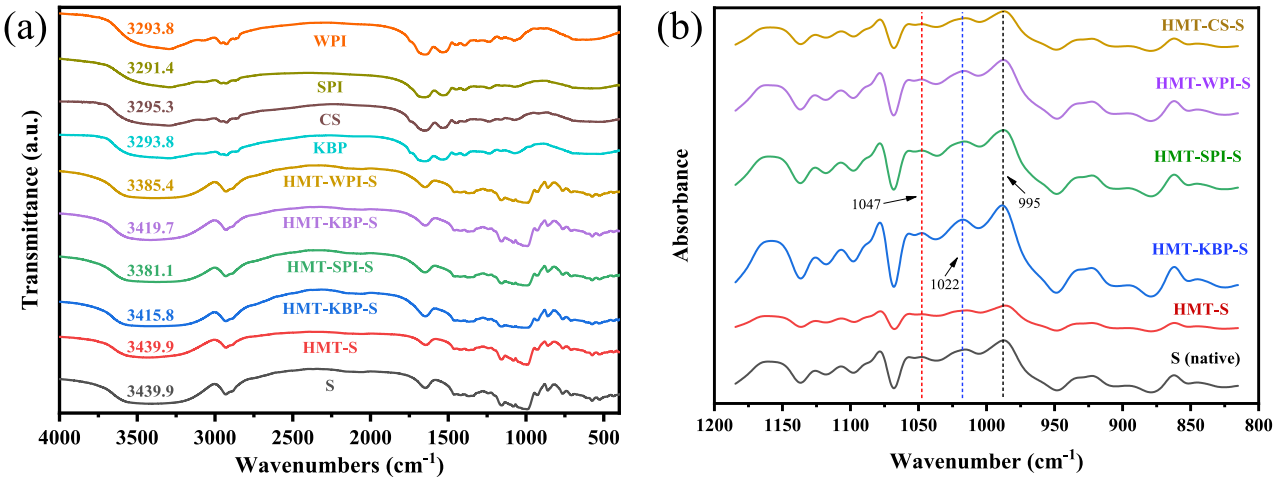

Fig. 3. (a) FTIR spectra of samples; (b) The deconvoluted FTIR spectra of S, HMT-S and complexes.

Table 1
Short-range orderliness, pasting characteristics, and the content of leached amylose of samples.

Samples	R_1	R_2	PT (°C)	PV (BU)	BD (BU)	SB (BU)	Leached amylose (mg/g)
S	0.780 ± 0.001^{bc}	0.788 ± 0.001^{c}	79.8 ± 0.3^{e}	194.3 ± 1.5^{a}	37.3 ± 2.1^{a}	143.0 ± 1.0^{a}	11.30 ± 0.19^{a}
HMT-S	0.766 ± 0.003^{d}	0.778 ± 0.002^{d}	86.6 ± 0.1^{b}	83.7 ± 0.6^{d}	0.3 ± 0.6^{d}	32.0 ± 1.7^{e}	6.53 ± 0.22^{c}
HMT-KBP-S	0.783 ± 0.003^{ab}	0.813 ± 0.000^{a}	85.1 ± 0.6^{c}	92.3 ± 1.5^{c}	1.3 ± 0.6^{cd}	34.7 ± 1.5^{d}	8.97 ± 0.56^{b}
HMT-SPI-S	0.789 ± 0.004^{a}	0.786 ± 0.001^{c}	81.4 ± 0.1^{d}	121.3 ± 0.6^{b}	5.3 ± 0.6^{b}	42.7 ± 0.6^{b}	10.80 ± 0.11^{a}
HMT-CS-S	0.774 ± 0.006^{cd}	0.797 ± 0.006^{b}	87.9 ± 0.1^{a}	62.7 ± 0.6^{e}	3.3 ± 1.2^{bc}	30.7 ± 1.5^{e}	7.05 ± 0.10^{c}
HMT-WPI-S	0.786 ± 0.005^{ab}	0.780 ± 0.002^{d}	84.7 ± 0.1^{c}	93.0 ± 1.0^{c}	2.7 ± 0.6^{c}	37.7 ± 0.6^{c}	8.83 ± 0.13^{b}

Note: All values are mean ± standard deviation and different letters in the same column are significantly different at $P < 0.05$ by ANOVA analysis.

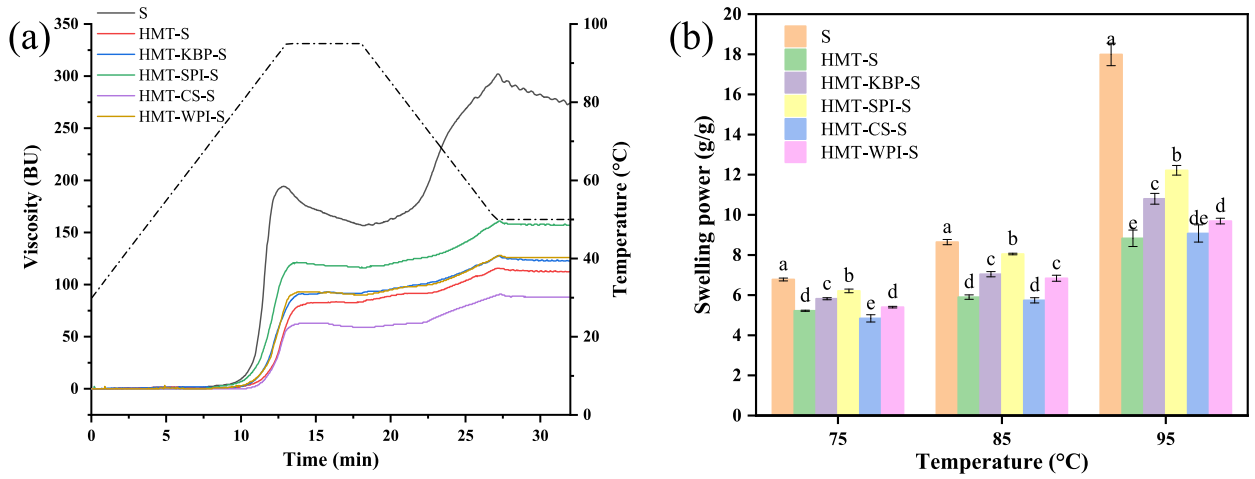

Fig. 4. (a) Pasting profiles of samples; (b) Swelling power of the samples at different temperatures.

optical birefringence and gel formation [38,39]. Starch/protein-water suspension consists of free and bound water, amylose, amylopectin, minerals, lipids and proteins. Therefore, the viscosity of the composite system reflects the interaction between the components during heating and shearing [40].

Compared to S, HMT-S exhibits an increase in PT and significant reductions in PV, BD, and SB. The changes can be attributed to two reasons. Firstly, the enhanced mobility of starch molecular chains under the influence of HMT facilitates their rearrangement and reorganization into ordered double-helical amylopectin clusters [41]. This rigid structure restricts starch swelling and enhances its stability during heating. Secondly, thermal energy facilitates the cleavage of long amylopectin chains during the HMT process. The subsequent interactions between the short chains and amylose enhance hydrogen bonding, reducing amylose leaching [42,43]. This, in turn, improves the heat resistance of starch and results in decreased starch viscosity. However, the effects of HMT on the paste viscosity of starch can vary, depending on factors such as starch source, instrumentation used, and HMT conditions [44].

According to previous experiments, adding 20 % protein to the physical mixture causes the viscosity of the entire system to decrease. The decrease in starch effective concentration in the continuous phase leads to the decrease in viscosity of the whole system. At the same time, these proteins can also act as plasticizers, inhibit the leaching and rearrangement of amylose molecules in starch paste, and reduce the viscosity of the system [45]. Different types of proteins have different degrees of viscosity reduction [46]. In this study, due to the high thermal stability of CS such that it is less likely to form micelles in hydrothermal environments, it exists as insoluble solid particles in the paste and reduces the viscosity of the paste. At the same time, the interaction between CS and starch may lead to the structural enhancement of CS, both of which result in HMT-CS-S having the lowest viscosity among all samples. This is consistent with the results of Chen et al. [16], where heat moisture treatment corn starch has the lowest viscosity compared to moist heat corn starch-soybean peptide complexes. From this, it can be seen that the effect of HMT on starch viscosity is greater than that of protein addition.

The BD value reflects the thermal stability of the starch paste, which is related to the swelling of the starch granules during the pasting process [35]. The BD value for all HMT samples decreased significantly. The results showed that HMT could decrease the viscosity of paste and improve its thermal stability and shear resistance. SB value represents the recrystallization degree of starch paste during the cooling process, which is related to short-term retrogradation caused by molecular rearrangement of amylose [23]. It reflects the stability and aging trend of cold starch paste. The data in Table 1 shows that the SB value of HMT-S and complex is lower than S ($P < 0.05$). HMT promotes amylose-amylose and/or amylopectin-amylopectin chain interactions, thereby reducing amylose leaching and short-term retrogradation, resulting in SB reduction of HMT samples [16].

3.6. Leached amylose content

During heating, starch granules will swell and eventually break due to the infiltration of a large number of water molecules, releasing part of amylose [35]. Table 1 shows the amylose leaching content of different samples. Among them, the amylose leaching content of samples treated with HMT decreased significantly. During the HMT process, some starch undergoes pasting, and amylose molecules will form a denser structure in the subsequent retrogradation process, thus inhibiting the leaching of amylose during the pasting process [27]. The magnitude relationship of the amount of amylose leached from each sample was in the following order: HMT-S < HMT-CS-S < HMT-WPI-S < HMT-KBP-S < HMT-SPI-S < S. This trend is consistent with Brabender viscosity. Among all the HMT samples, HMT-S had the lowest amylose leaching (6.53 ± 0.22 mg/g). However, the addition of protein increases amylose leaching. Most studies have found that the interaction between starch and protein reduces the amount of amylose leaching during the pasting process [35,47,48]. But Wang et al. [49] found that acidic amino acids (Asp and

Glu) can reduce the swelling ability of starch, but increase the leaching of linear starch. However, in this study, the composition of amino acids was clearly insufficient to support the explanation for the increase in amylose leaching. The moisture content in HMT has a significant impact on the properties of starch, and HMT samples with higher moisture content typically have lower SP and amylose leaching amounts [50,51]. Proteins with a large number of polar groups have higher hydrophilicity than starch, which leads to a decrease in the water content of starch used for HMT in protein containing systems. Therefore, compared with HMT-S, the addition of protein resulted in an increase in the amount of amylose leaching from the complex.

3.7. Swelling power (SP)

SP is an index to measure the ability of starch granules to absorb water during the heating process, which reflects the degree of interaction between starch particles and water molecules. Fig. 4(b) shows the SP of S, HMT-S and four protein-starch complexes. It can be observed from the figure that the SP of all samples shows an upward trend with the increase in temperature. SP did not change significantly between samples in the incubation temperature range below 85 °C, probably because most starch samples had not reached pasting temperature. This inference was supported by PT values for pasting properties of samples. In particular, it should be noted that when the incubation temperature reached 85 °C, the PT value of S was exceeded. At this temperature, heating S suspension will cause starch granules to swell, which is conducive to the penetration of water molecules into the granules, thus significantly increasing the SP of S. The SP of samples subjected to HMT was generally lower than S under different incubation temperature conditions. This can be attributed to the rearrangement of starch molecular chains during HMT, resulting in increased interaction between functional groups involved in starch bonding [52]. Additionally, the formation of a more ordered set of double helical branched side chains increases the rigidity of this structure, which limits water absorption and swelling of starch granules [42]. This finding is consistent with the results of the samples pasting properties described in Section 3.5.

Sun et al. [53] proposed that the swelling of starch is mainly driven by its amylopectin. Meanwhile, amylose acts as a diluent and swelling inhibitor in starch granules and can maintain the integrity of starch swelling granules. This study found that the effect of protein-starch complexes on SP under different temperature conditions is highly consistent with the leaching behavior of amylose. The SP differences between protein-starch complexes may be due to the differences in protein structure, in which the differences in hydrophilic/hydrophobic groups in proteins affect the interaction between protein and starch and then act on SP [49]. Interestingly, HMT-CS-S exhibits the lowest SP among the four different complexes at all temperature gradients. Meanwhile, we found in our experiments that CS mainly exists in the form of insoluble particles in the paste. This may be due to the thermal stability and surface hydrophobicity of CS. In contrast, the gelation of KBP, SPI and WPI in hydrothermal environments increased the SP of the whole system. HMT-CS-S also showed different trends in the pasting properties from the other complexes.

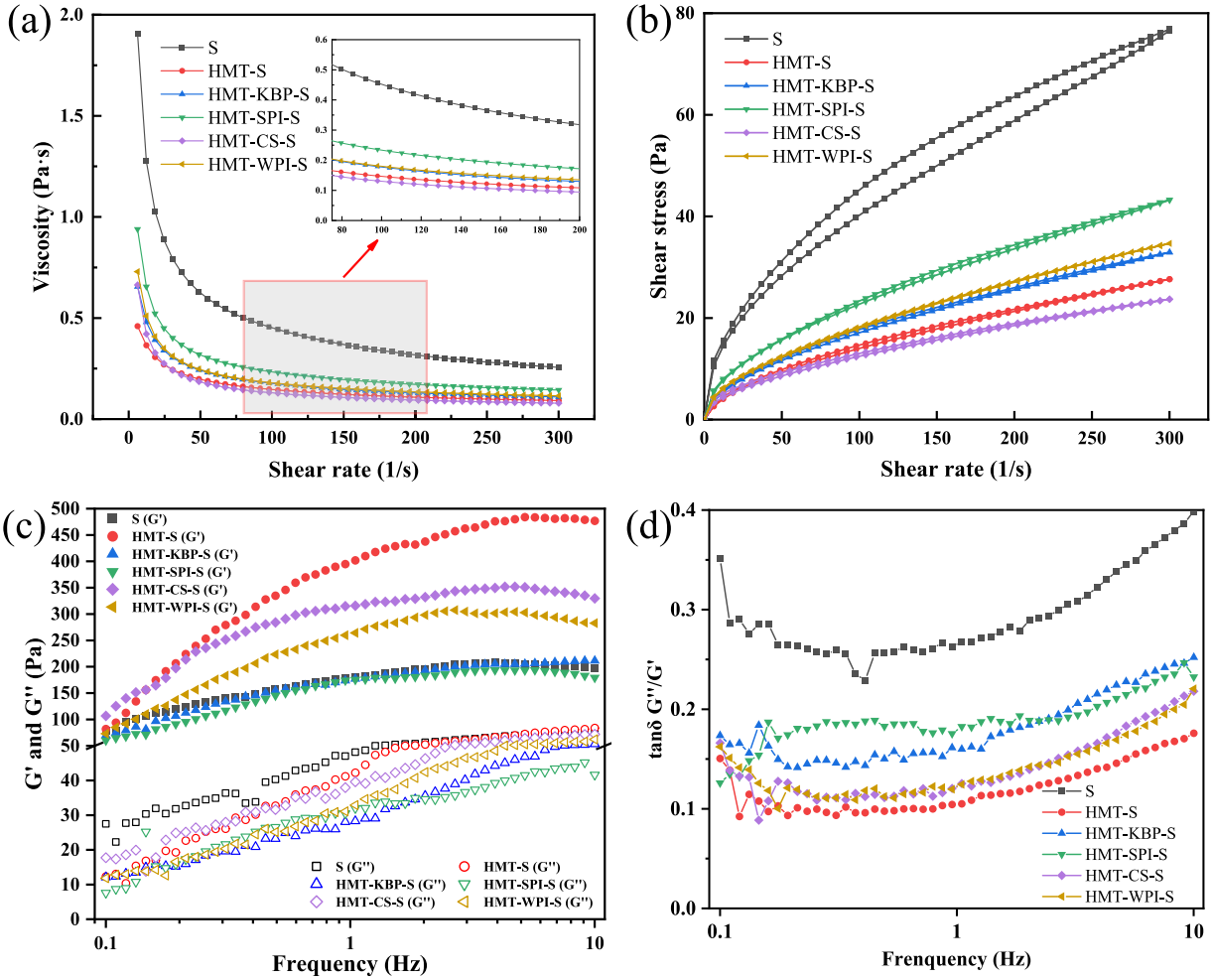

Fig. 5. Samples' (a) shear rate and viscosity; (b) shear rate and shear stress; (c) storage modules G' and loss modules G"; (d) tan δ.

3.8. Rheological analysis

3.8.1. Steady shear rheological analysis

Fig. 5(a) and (b) show the samples' viscosity-shear rate curve and shear stress-shear rate curve, respectively. When shear forces are applied, molecular chains change from their initial configuration, and entangled polymer segments unravel. This process reduces the interaction forces between the flow layers, leading to a decrease in apparent viscosity [49]. HMT-SPI-S has the highest viscosity (0.1443–0.9392 Pa·s), consistent with its maximum SB value in Section 3.5 compared to the other three protein-starch complexes. During starch retrogradation, swollen starch granules recombine with protein, increasing the system's viscosity [19].

Table 2 gives the fitting parameters of the power-law model for the steady-state flow curves of the sample rising and falling. The data in the table show that the determination coefficients (R^2) are all >0.99, indicating that the power-law equation fits well with the rheological curves of each sample paste. The coefficient of consistency (K) indicates the consistency of the material, the greater the value, the higher the consistency [24]. As both HMT and protein addition can limit the swelling of starch granules and amylose leaching, the consistency coefficient decreases. For HMT, the rearrangement of the starch chains forms a denser structure, which reduces the K value of the samples. For protein, hydrophilic groups on protein compete with starch for water on the one hand, and protein also wraps on the surface of starch granules to limit starch swelling. On the other hand, the interaction between protein and starch reduces the likelihood of amylose interacting with amylose [49].

The flow behavior index (n), sometimes called the power-law index, reflects the proximity to Newtonian fluids. When $n = 1$, corresponding to Newtonian fluid, the lower the n value, the higher the pseudoplastic degree of the paste. As seen from the data in Table 2, all the sample pastes have n values <1, indicating that all the starch pastes tend to be non-Newtonian fluids with pseudoplastic behavior. At rest, starch polymer chains entangle and form stable molecular structures. Under shear, the conformation of molecular chains changes and the entangled polymer segments are opened. This leads to a decrease in the internal resistance of paste and shear thinning, which leads to a pseudoplastic phenomenon [54].

The area of the hysteresis loop reflects the degree of thixotropy. The larger the hysteresis loop, the greater the thixotropy [24]. After HMT, the hysteresis loop area of samples decreased significantly from 1106.1108 ± 19.6444 Pa·s^{-1} to <200 Pa·s^{-1} for all samples. This shows that the shear stability of the HMT-prepared samples was improved, and the HMT sample system forms a relatively stable structure. This also explains the high enzymatic resistance of HMT samples [13]. Interestingly, the hysteresis loop area of HMT-WPI-S is negative, which indicates that the system was destroyed in the upward and downward shear processes.

3.8.2. Dynamic rheological analysis

The dynamic rheological test results of the samples are shown in Fig. 5(c-d), where the energy storage modulus (G') represents the elasticity and strength of the gel structure, while the loss modulus (G") reflects the viscosity and fluidity of the gel structure [9]. Throughout the entire frequency range, G' and G" of all samples increase with increasing frequency. Compared with S, HMT-S has a higher G', indicating that the gel strength of HMT-S is enhanced after HMT. Yang et al. [55] suggested that HMT may lead to the degradation of starch molecular chains, which facilitates the rearrangement between starch molecules and allows starch molecules to form a continuous gel network structure, thus enhancing its gel strength. Under HMT conditions, the presence of protein decreased the G' value of the complex compared to S. This agrees with the study of Zhang et al. [9], who concluded that with limited protein supplementation, the mutual binding and entanglement between starch and protein prevent amylose from binding to each other, weakening starch gel elasticity. It can be seen from Fig. 5(c) that SPI has the greatest effect on the G" value after adding different proteins to HMT, and a lower G" value indicates that the viscosity of the complex decreases, which is consistent with the results of Brabender viscosity. This difference may be closely related to the distribution behavior of protein in the starch matrix, which will be discussed in the following LF-NMR analysis.

tan δ is the ratio of G" and G', since G' is larger than G", indicating that the elastic properties of the composite are better than the viscosity properties, which are closer to solid than liquid. This means the gel is more structurally stable, holds its shape better and is less likely to flow. Due to tan δ < 1, all complexes exhibit a typical weak gel structure. The tan δ of all the samples increases with increasing frequency, where the tan δ of S varies relatively more significantly with a distribution between 0.25 and 0.4. In contrast, the samples show less variation. In the HMT samples, the tan δ of the HMT-KBP-S complex is larger, indicating that the HMT-KBP-S system is more mobile, and the more the sample paste resembles liquid [19]. The control sample S has the highest tan δ, which is consistent with the results of SP, that is, S has the highest water-holding capacity.

3.9. LF-NMR analysis

The spin-spin relaxation time (T_2) derived from LR-NMR is closely related to water mobility. A decrease in T_2 means that water is less mobile and binds more tightly to the matrix, thereby increasing the water-holding capacity of the sample. T_2 is subdivided into T_{21}, T_{22}, and T_{23}, corresponding to tightly bound water, weakly bound water, and free water, respectively. A_{21}, A_{22} and A_{23} quantify their respective contents [56]. The effect of different proteins on the water-holding capacity of the system is shown in Table 3 and Fig. 6. There are three types of water in all samples, among which free water is the dominant component.

The peak area distributions of A_{21}, A_{22} and A_{23} for native starch gel were 0.47 %, 3.05 % and 96.48 %, while the peak areas of A_{21} and A_{23} for HMT-S increased to 0.72 % and 96.81 %, respectively, while the peak area of A_{22} decreased slightly to 2.48 %. When the native starch was pasted, the amylose leaching rate increased, and amylose leached easily entangled to form a sticky starch paste. This limits the mobility of water molecules in the samples. Under high temperature and high humidity HMT conditions, part of the starch gelatinization was mainly concentrated on the surface of the starch granules. And in the subsequent

Table 2
Fitting parameters for the Ostwald de Waele equation for samples.

Sample	Ascending curve			Descending curve			Thixotropic area/(Pa·s^{-1})
	K/(Pa·S^n)	n_1	R^2	K/(Pa·S^n)	n_2	R^2	
S	4.4870 ± 0.0937^a	0.4998 ± 0.0021^c	0.9999	4.6615 ± 0.9592^a	0.4785 ± 0.0409^c	0.9977	1106.1108 ± 19.6444^a
HMT-S	1.1307 ± 0.1132^d	0.5613 ± 0.0005^a	0.9999	1.0000 ± 0.0000^c	0.5792 ± 0.0203^a	0.9996	144.9145 ± 14.9296^b
HMT-KBP-S	1.4585 ± 0.0269^c	0.5441 ± 0.0031^b	0.9999	1.2830 ± 0.0146^{bc}	0.5652 ± 0.0014^{ab}	0.9999	133.9630 ± 6.4601^b
HMT-SPI-S	2.0088 ± 0.0612^b	0.5354 ± 0.0084^b	0.9999	1.9390 ± 0.0822^b	0.5385 ± 0.0067^b	0.9997	167.6346 ± 37.0083^b
HMT-CS-S	1.4527 ± 0.0660^c	0.4826 ± 0.0100^d	0.9994	1.1252 ± 0.0263^c	0.5275 ± 0.0140^b	0.9995	132.2104 ± 21.0528^b
HMT-WPI-S	1.5072 ± 0.0637^c	0.5443 ± 0.0008^b	0.9996	1.5004 ± 0.0315^{bc}	0.5466 ± 0.0033^{ab}	0.9998	−45.4109 ± 5.1224^c

Note: All values are mean ± standard deviation and different letters in the same column are significantly different at $P < 0.05$ by ANOVA analysis.

Table 3
The transverse relaxation time (T_2) and related peak area (A_2) of all sample gels.

Samples	Peak time (ms)			Peak area ratio (%)		
	T_{21}	T_{22}	T_{23}	A_{21}	A_{22}	A_{23}
S	2.34 ± 0.20^{d}	5.00 ± 0.14^{c}	139.96 ± 3.97^{d}	0.47 ± 0.23^{c}	3.05 ± 0.20^{bc}	96.48 ± 0.03^{a}
HMT-S	2.97 ± 0.17^{c}	6.37 ± 0.52^{c}	155.22 ± 3.85^{c}	0.72 ± 0.06^{c}	2.48 ± 0.28^{c}	96.81 ± 0.55^{a}
HMT-KBP-S	5.74 ± 0.16^{a}	15.19 ± 4.52^{b}	166.38 ± 0.00^{b}	2.04 ± 0.81^{b}	3.31 ± 0.69^{b}	94.66 ± 0.11^{b}
HMT-SPI-S	4.84 ± 0.27^{b}	16.27 ± 0.46^{b}	172.36 ± 4.88^{b}	1.81 ± 0.03^{b}	5.00 ± 0.03^{a}	93.18 ± 0.06^{c}
HMT-CS-S	–	6.08 ± 0.20^{c}	83.23 ± 4.72^{e}	–	3.60 ± 0.10^{b}	96.40 ± 0.25^{a}
HMT-WPI-S	5.36 ± 0.15^{a}	20.73 ± 0.00^{a}	219.64 ± 0.00^{a}	2.84 ± 0.17^{a}	2.65 ± 0.18^{c}	94.51 ± 0.01^{b}

Note: All values are mean ± standard deviation and different letters in the same column are significantly different at $P < 0.05$ by ANOVA analysis.

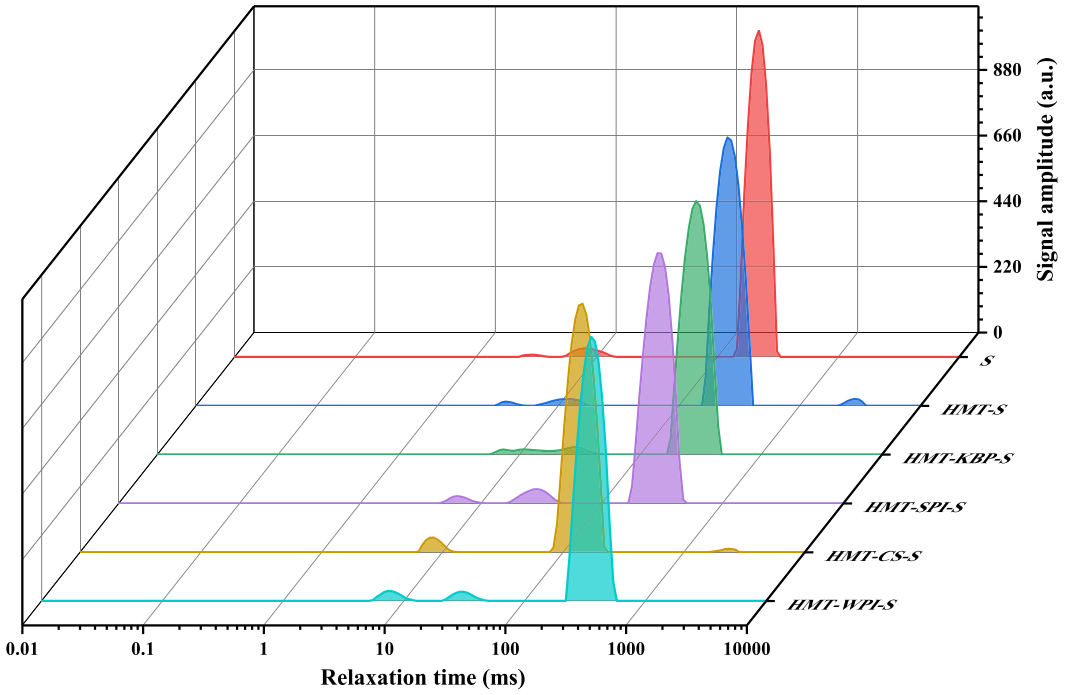

Fig. 6. The transverse relaxation time spectrum of LF-NMR of all sample gels.

cooling process, the gelatinized starch retrograded to form a dense shell. At the same time, heat treatment also led to the change of protein conformation. The protein layer increased starch surface hydrophobicity and decreased starch granule swelling [57]. This thereby leads to a reduction in amylose leaching, which is consistent with the results of section 3.6 on amylose leaching.

Different exogenous proteins affected the water distribution of starch gels to different degrees, but the trend of the effects was the same. In addition to CS, adding proteins resulted in an increase in bound water and a decrease in free water in the complex gels. The A_{23} peak area decreased to 94.66 % (HMT-KBP-S), 93.18 % (HMT-SPI-S) and 94.51 % (HMT-WPI-S), respectively. The change in water mobility of the HMT samples system showed that proteins could compete with starch for water during the pasting process, limiting starch granule swelling while inhibiting starch digestion. The different characteristics of protein give it different distribution behaviors in the starch matrix and then affect the system's water distribution. By FTIR analysis (Table S1), KBP with more β-turns and random coil had a lower structural density, which may lead to easier unfolding of the structure of KBP during pasting and the reformation of larger aggregates during cooling [9]. These aggregates limit starch swelling by occupying available space in the system, thus inhibiting starch digestion. SPI and WPI form a dense network structure, and this barrier effect will limit the water absorption and swelling of starch. In addition, the enhancement of water holding capacity of the system after adding protein may be related to two reasons. On the one hand, the non-covalent interaction between protein and starch indirectly leads to more exposure to hydroxyl groups in starch, which is conducive to binding free water molecules, and this part forms a part of weakly bound water[36]. On the other hand, polar groups in protein molecules (such as hydroxyl and carboxyl groups) interact with water molecules to form hydrogen bonds, limiting the movement of water and thereby increasing the bound water content [36].

3.10. The mechanism of protein on starch digestion under HMT

Many factors affect starch digestibility, including starch source, particle size, degree of polymerization, starch structure, processing conditions, endogenous/exogenous proteins, lipids and other elements [3]. Fig. 7 illustrates the mechanism of protein inhibition of starch digestion under HMT. Starch can be categorized into amylose and amylopectin, with amylopectin having a cluster structure. During HMT, the amylopectin side chain clusters were detached from the starch backbone due to the effects of water, heat, and pressure. This separation removes spatial constraints and confers higher flexibility to side chain clusters, resulting in tighter rearrangements [58]. This results in the surface of starch particles becoming hydrophobic and endows them with greater rigidity and resistance to rapid heating by changing their swelling behavior [57,59]. As a result, the hydrophobicity of the surface of the HMT samples led to a decrease in the viscosity of the system compared to the native starch (Fig. 4a). At the same time, the formation

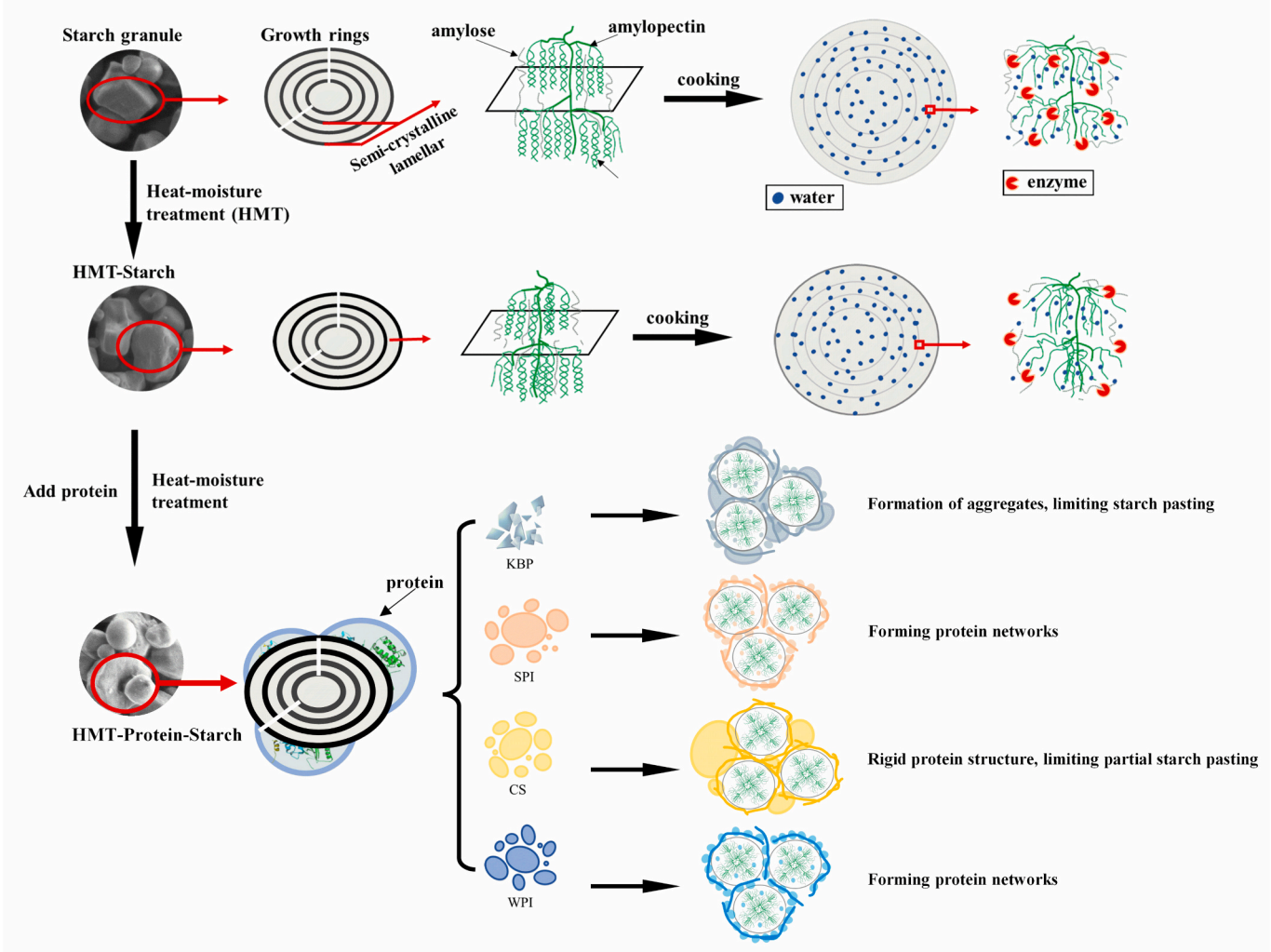

Fig. 7. The mechanism of proteins inhibition of starch digestion under heat-moisture treatment (HMT).

of a rigid structure resulted in reduced leaching of amylose (Table 1) and reduced swelling power (Fig. 4b). The formation of a dense starch structure increased the resistance to enzymatic digestion (higher RDS and RS content).

Adding protein to the HMT process will further reduce the digestibility of starch. Proteins wrap around the surface of starch particles or embed starch particles into the protein matrix (Fig. 2), acting as physical barriers to hinder enzyme digestion of starch. Except for CS, the other three proteins inhibited α-amylase activity (Fig. S1). During the pasting process of HMT-KBP-S, the relatively loose KBP structure unfolds, and in the subsequent cooling process, it reaggregates to form larger aggregates, which occupy adequate space and limit starch expansion, thereby reducing starch digestibility. SPI and WPI form a network structure in their respective systems, with WPI having a denser structure forming a more robust network structure. Meanwhile, adding protein can enhance the ordered structure of starch disrupted by HMT (Table 1). Under the synergistic effect of HMT and exogenous proteins, starch digestibility in the complex system is significantly reduced.

4. Conclusion

This paper investigated the effect of adding proteins from different sources (KBP, SPI, CS, and WPI) on the structure, physicochemical properties and *in vitro* digestibility of corn starch under heat-moisture treatment (HMT). The results showed that HMT could significantly enhance the rigid structure of starch, inhibit its pasting and short-term retrogradation, and effectively limit starch swelling and amylose leaching. At the same time, HMT also improved the thermal stability and shear resistance of starch samples in the paste state. The addition of exogenous proteins further reduced starch digestibility. Among them, HMT-KBP-S showed the lowest C_∞ value in the uncooked and cooked states, indicating strong anti-digestibility. In addition, except for casein, the other three proteins effectively inhibit the activity of α-amylase, thus slowing down the digestion process of starch. The inhibitory effects were in the order of KBP ($IC_{50} = 1.712 \pm 0.085$ mg/mL) > SPI ($IC_{50} = 1.949 \pm 0.107$ mg/mL) > WPI ($IC_{50} = 2.083 \pm 0.146$ mg/mL). The inclusion of proteins also improved the short-range ordering of the starch and increased its resistance to enzymatic degradation. In the complexes with dense protein structures, starch granules are embedded in the protein matrix. In contrast, in loose protein (KBP), protein wraps around the surface of starch granules, acting as a physical barrier to hinder starch digestion. Rheological differences and the increase in water-holding capacity are closely related to the distribution behavior of proteins in the starch matrix. Aggregates or network structures formed by different proteins can effectively limit starch's water absorption and swelling, thus reducing the accessibility of enzymes to starch. These results provide a new idea for reducing starch digestibility and a theoretical basis for designing low glycemic index foods. Future studies could further explore the effects of different protein hydrolysates on starch digestibility under different heat treatment conditions to more comprehensively understand the protein-starch interactions and their influence on starch digestion.

CRediT authorship contribution statement

Xiuli Wu: Writing – review & editing, Supervision, Resources, Formal analysis. **Xuexu Wu:** Writing – original draft, Investigation, Data curation. **Jianwen Zhang:** Writing – review & editing, Data curation. **Xiangxuan Yan:** Writing – review & editing, Methodology. **Qing Zhang:** Writing – review & editing, Methodology. **Bingqian Zhang:** Investigation.

Declaration of competing interest

The authors declare that they have no known competing financial interests or personal relationships that could have appeared to influence the work reported in this paper.

Data availability

Data will be made available on request.

Acknowledgments

This research was supported by the Enterprise Commissioned Technology Development Program (2023JBH26L50).

Appendix A. Supplementary data

Supplementary data to this article can be found online at https://doi.org/10.1016/j.ijbiomac.2024.133079.

References

[1] T. Wang, X.B. Yang, D.Y. Wang, Y.D. Jiao, Y. Wang, Y. Zhao, Analysis of compositional carbohydrates in polysaccharides and foods by capillary zone electrophoresis, Carbohydr. Polym. 88 (2) (2012) 754–762, https://doi.org/10.1016/j.carbpol.2012.01.039.

[2] H.N. Englyst, S.M. Kingman, J.H. Cummings, Classification and measurement of nutritionally important starch fractions, Eur. J. Clin. Nutr. 46 (1992) S33–S50.

[3] X.X. Lu, R.R. Ma, J.L. Zhan, F. Wang, Y.Q. Tian, The role of protein and its hydrolysates in regulating the digestive properties of starch: a review, Trends Food Sci. Technol. 125 (2022) 54–65, https://doi.org/10.1016/j.tifs.2022.04.027.

[4] X. Wu, H. Yu, G. Bao, M. Luan, C. Wang, Preparation of adzuki bean starch-lipid complexes and their anti-digestion mechanism, J. Food Meas. Charact. 16 (2) (2022) 945–956, https://doi.org/10.1007/s11694-021-01222-z.

[5] J.J. Cai, C. Chao, B. Niu, L. Copeland, J.L. Yu, S. Wang, S.J. Wang, New insight into the interactions among starch, lipid and protein in model systems with different starches, Food Hydrocoll. 112 (2021) 106323, https://doi.org/10.1016/j.foodhyd.2020.106323.

[6] B.J. Zhang, D.L. Qiao, S.M. Zhao, Q.L. Lin, J. Wang, F.W. Xie, Starch-based food matrices containing protein: recent understanding of morphology, structure, and properties, Trends Food Sci. Technol. 114 (2021) 212–231, https://doi.org/10.1016/j.tifs.2021.05.033.

[7] N. López-Barón, Y.C. Gu, T. Vasanthan, R. Hoover, Plant proteins mitigate *in vitro* wheat starch digestibility, Food Hydrocoll. 69 (2017) 19–27, https://doi.org/10.1016/j.foodhyd.2017.01.015.

[8] J. Wang, S.M. Zhao, G. Min, D.L. Qiao, B.J. Zhang, M. Niu, C.H. Jia, Y. Xu, Q.L. Lin, Starch-protein interplay varies the multi-scale structures of starch undergoing thermal processing, Int. J. Biol. Macromol. 175 (2021) 179–187, https://doi.org/10.1016/j.ijbiomac.2021.02.020.

[9] S.H. Zhang, S. Zhu, F. Zhong, D.J. Huang, X.M. Chen, Y. Li, Study on the mechanism of various exogenous proteins with different inhibitions on wheat starch digestion: from the distribution behaviors of protein in the starch matrix, Int. J. Biol. Macromol. 242 (2023) 124909, https://doi.org/10.1016/j.ijbiomac.2023.124909.

[10] N. López-Barón, D. Sagnelli, A. Blennow, M. Holse, J. Gao, L. Saaby, A. Müllertz, B. Jespersen, T. Vasanthan, Hydrolysed pea proteins mitigate *in vitro* wheat starch digestibility, Food Hydrocoll. 79 (2018) 117–126, https://doi.org/10.1016/j.foodhyd.2017.12.009.

[11] X. Chen, X.W. He, B. Zhang, L.J. Sun, Z.L. Liang, Q. Huang, Wheat gluten protein inhibits α-amylase activity more strongly than a soy protein isolate based on kinetic analysis, international, Int. J. Biol. Macromol. 129 (2019) 433–441, https://doi.org/10.1016/j.ijbiomac.2019.01.215.

[12] J. Zhu, X. Chen, J.W. Luo, Y.J. Liu, B. Wang, Z.L. Liang, L. Li, Insight into the binding modes and mechanisms of inhibition between soybean-peptides and α-amylase based on spectrofluorimetry and kinetic analysis, LWT Food Sci. Technol. 142 (2021) 110977, https://doi.org/10.1016/j.lwt.2021.110977.

[13] X.X. Lu, J.L. Zhan, R.R. Ma, Y.Q. Tian, Structure, thermal stability, and *in vitro* digestibility of rice starch–protein hydrolysate complexes prepared using different hydrothermal treatments, Int. J. Biol. Macromol. 230 (2023) 123130, https://doi.org/10.1016/j.ijbiomac.2022.123130.

[14] D. Zia ud, H.G. Xiong, P. Fei, Physical and chemical modification of starches: a review, Crit. Rev. Food Sci. Nutr. 57 (12) (2017) 2691–2705, https://doi.org/10.1080/10408398.2015.1087379.

[15] L.M. Fonseca, S.L.M. El Halal, A.R.G. Dias, E.D. Zavareze, Physical modification of starch by heat-moisture treatment and annealing and their applications: a review, Carbohydr. Polym. 274 (2021) 118665, https://doi.org/10.1016/j.carbpol.2021.118665.

[16] X. Chen, J.W. Luo, L.L. Fu, D.Z. Cai, X.Y. Lu, Z.L. Liang, J. Zhu, L. Lia, Structural, physicochemical, and digestibility properties of starch-soybean peptide complex subjected to heat moisture treatment, Food Chem. 297 (2019) 124957, https://doi.org/10.1016/j.foodchem.2019.124957.

[17] T. Liu, Y. Gu, A.L.A. Waleed, L. Wang, Y. Li, H. Qian, Challenges and opportunities in developing low glycemic index foods with white kidney bean α-amylase inhibitor, Trends Food Sci. Technol. 147 (2024) 104397, https://doi.org/10.1016/j.tifs.2024.104397.

[18] S.Y. Jia, B. Yu, H.B. Zhao, H.T. Tao, P.F. Liu, B. Cui, Physicochemical properties and *in vitro* digestibility of dual-modified starch by cross-linking and annealing, Starch-Stärke 74 (1-2) (2022) 2100102, https://doi.org/10.1002/star.202100102.

[19] Y.Y. Ding, J.J. Cheng, Q.Y. Lin, Q.Y. Wang, J.R. Wang, G.P. Yu, Effects of endogenous proteins and lipids on structural, thermal, rheological, and pasting properties and digestibility of adlay seed (*Coix lacryma-jobi* L.) starch, Food Hydrocoll. 111 (2021) 106254, https://doi.org/10.1016/j.foodhyd.2020.106254.

[20] N. Sun, J.Y. Xie, B. Zheng, J.H. Xie, Y. Chen, X.B. Hu, Q. Yu, The inhibition mechanism of bound polyphenols extracted from mung bean coat dietary fiber on porcine pancreatic α-amylase: kinetic, spectroscopic, differential scanning calorimetric and molecular docking, Food Chem. 436 (2024) 137749, https://doi.org/10.1016/j.foodchem.2023.137749.

[21] P.T. Akonor, C.O. Tutu, W. Arthur, J. Adjebeng-Danquah, N.S. Affrifah, A.S. Budu, F.K. Saalia, Granular structure, physicochemical and rheological characteristics of starch from yellow cassava (*Manihot esculenta*) genotypes, Int. J. Food Prop. 26 (1) (2023) 259–273, https://doi.org/10.1080/10942912.2022.2161572.

[22] X.L. Wu, M.R. Luan, X.X. Yan, J.W. Zhang, X.X. Wu, Q. Zhang, The impact of different concentrations of hyaluronic acid on the pasting and microstructural properties of corn starch, Int. J. Biol. Macromol. 254 (2024) 127555, https://doi.org/10.1016/j.ijbiomac.2023.127555.

[23] Y. Hu, C.X. He, M.Y. Zhang, L.Q. Zhang, H. Xiong, Q. Zhao, Inhibition from whey protein hydrolysate on the retrogradation of gelatinized rice starch, Food Hydrocoll. 108 (2020) 105840, https://doi.org/10.1016/j.foodhyd.2020.105840.

[24] A.R. Górecki, W. Blaszczak, J. Lewandowicz, J. Le Thanh-Blicharz, K. Penkacik, Influence of high pressure or autoclaving-cooling cycles and pullulanase treatment on buckwheat starch properties and resistant starch formation, Pol. J. Food Nutr. Sci. 68 (3) (2018) 235–242, https://doi.org/10.1515/pjfns-2018-0001.

[25] C.F. Li, P.P. Cao, P. Wu, W.W. Yu, R.G. Gilbert, E.P. Li, Effects of endogenous proteins on rice digestion during small intestine (*in vitro*) digestion, Food Chem. 344 (2021) 128687, https://doi.org/10.1016/j.foodchem.2020.128687.

[26] T.H. Vu, S. Bean, C.F. Hsieh, Y.C. Shi, Changes in protein and starch digestibility in sorghum flour during heat-moisture treatments, J. Sci. Food Agric. 97 (14) (2017) 4770–4779, https://doi.org/10.1002/jsfa.8346.

[27] H.W. Wang, Y.F. Liu, L. Chen, X.X. Li, J. Wang, F.W. Xie, Insights into the multi-scale structure and digestibility of heat-moisture treated rice starch, Food Chem. 242 (2018) 323–329, https://doi.org/10.1016/j.foodchem.2017.09.014.

[28] H.J. Chung, D.W. Cho, J.D. Park, D.K. Kweon, S.T. Lim, *In vitro* starch digestibility and pasting properties of germinated brown rice after hydrothermal treatments, J. Cereal Sci. 56 (2) (2012) 451–456, https://doi.org/10.1016/j.jcs.2012.03.010.

[29] M.Z. Zheng, Y. Xiao, S. Yang, M.H. Liu, L. Feng, Y.H. Ren, X.B. Yang, N. Lin, J. S. Liu, Effect of adding zein, soy protein isolate and whey protein isolate on the physicochemical and *in vitro* digestion of proso millet starch, Int. J. Food Sci. Technol. 55 (2) (2020) 776–784, https://doi.org/10.1111/ijfs.14347.

[30] X. Chen, X.W. He, B. Zhang, X. Fu, J.L. Jane, Q. Huang, Effects of adding corn oil and soy protein to corn starch on the physicochemical and digestive properties of the starch, Int. J. Biol. Macromol. 104 (2017) 481–486, https://doi.org/10.1016/j.ijbiomac.2017.06.024.

[31] W.W. Yu, W. Zou, S. Dhital, P. Wu, M.J. Gidley, G.P. Fox, R.G. Gilbert, The adsorption of α-amylase on barley proteins affects the *in vitro* digestion of starch in barley flour, Food Chem. 241 (2018) 493–501, https://doi.org/10.1016/j.foodchem.2017.09.021.

[32] Z.Q. Wang, M.C. Fan, K. Hannachi, Y. Li, H.F. Qian, L. Wang, Impact of red kidney bean protein on starch digestion and exploring its underlying mechanism, Int. J. Biol. Macromol. 253 (2023) 127023, https://doi.org/10.1016/j.ijbiomac.2023.127023.

[33] D. Dong, B. Cui, Fabrication, characterization and emulsifying properties of potato starch/soy protein complexes in acidic conditions, Food Hydrocoll. 115 (2021) 106600, https://doi.org/10.1016/j.foodhyd.2021.106600.

[34] M.D. Fernández-Alonso, D. Díaz, M.A. Berbis, F. Marcelo, J. Cañada, J. Jiménez-Barbero, Protein-carbohydrate interactions studied by NMR: from molecular recognition to drug design, Curr. Protein Pept. Sci. 13 (8) (2012) 816–830, https://doi.org/10.2174/138920312804871175.

[35] H.Y. Bao, Q. Liu, Y.Y. Yang, L.L. Xu, K.F. Zhu, Z.Y. Jin, A.Q. Jiao, Effects of rice protein, soy isolate protein, and whey concentrate protein on the digestibility and physicochemical properties of extruded rice starch, J. Food Sci. 88 (3) (2023) 1159–1171, https://doi.org/10.1111/1750-3841.16458.

[36] L. Lin, X.T. Yu, Y.C. Gao, L.P. Mei, Z.J. Zhu, X.F. Du, Physicochemical properties and *in vitro* starch digestibility of wheat starch/rice protein hydrolysate complexes,

Food Hydrocoll. 125 (2022) 107348, https://doi.org/10.1016/j.foodhyd.2021.107348.
[37] Y.X. Zhong, X.X. Yin, Y. Yuan, X.L. Kong, S.G. Chen, X.Q. Ye, J.H. Tian, Changes in physiochemical properties and *in vitro* digestion of corn starch prepared with heat-moisture treatment, Int. J. Biol. Macromol. 248 (2023) 125912, https://doi.org/10.1016/j.ijbiomac.2023.125912.
[38] B. Song, X.Y. Xu, J.Y. Hou, M.H. Liu, N. Yi, C.B. Zhao, J.S. Liu, Research on corn starch and black bean protein isolate interactions during gelatinization and their effects on physicochemical properties of the blends, Int. J. Biol. Macromol. 254 (2024) 127827, https://doi.org/10.1016/j.ijbiomac.2023.127827.
[39] N. Rincón-Londoño, L.J. Vega-Rojas, M. Contreras-Padilla, A.A. Acosta-Osorio, M. E. Rodríguez-García, Analysis of the pasting profile in corn starch: structural, morphological, and thermal transformations, part I, Int. J. Biol. Macromol. 91 (2016) 106–114, https://doi.org/10.1016/j.ijbiomac.2016.05.070.
[40] E.A. Esquivel-Fajardo, E.U. Martinez-Ascencio, M.E. Oseguera-Toledo, S. M. Londoño-Restrepo, M.E. Rodriguez-García, Influence of physicochemical changes of the avocado starch throughout its pasting profile: combined extraction, Carbohydr. Polym. 281 (2022) 119048, https://doi.org/10.1016/j.carbpol.2021.119048.
[41] X. Chen, X.W. He, X. Fu, Q. Huang, *In vitro* digestion and physicochemical properties of wheat starch/flour modified by heat-moisture treatment, J. Cereal Sci. 63 (2015) 109–115, https://doi.org/10.1016/j.jcs.2015.03.003.
[42] E.D. Zavareze, A.R.G. Dias, Impact of heat-moisture treatment and annealing in starches a review, Carbohydr. Polym. 83 (2) (2011) 317–328, https://doi.org/10.1016/j.carbpol.2010.08.064.
[43] B. Klein, V.Z. Pinto, N.L. Vanier, E.D. Zavareze, R. Colussi, J.A. do Evangelho, L. C. Gutkoski, A.R.G. Dias, Effect of single and dual heat-moisture treatments on properties of rice, cassava, and pinhao starches, Carbohydr. Polym. 98 (2) (2013) 1578–1584, https://doi.org/10.1016/j.carbpol.2013.07.036.
[44] R. Hormdok, A. Noomborm, Hydrothermal treatments of rice starch for improvement of rice noodle quality, LWT Food Sci. Technol. 40 (10) (2007) 1723–1731, https://doi.org/10.1016/j.lwt.2006.12.017.
[45] J.O. Narciso, C. Brennan, Whey and pea protein fortification of rice starches: effects on protein and starch digestibility and starch pasting properties, Starch-Stärke 70 (9-10) (2018) 1700315, https://doi.org/10.1002/star.201700315.
[46] C.R. Storck, E.D. Zavareze, M.A. Gularte, M.C. Elias, C.M. Rosell, A.R.G. Dias, Protein enrichment and its effects on gluten-free bread characteristics, LWT Food Sci. Technol. 53 (1) (2013) 346–354, https://doi.org/10.1016/j.lwt.2013.02.005.
[47] R. Bravo-Núñez, C.M. Garzón, M. Rosell, Gómez, evaluation of starch-protein interactions as a function of pH, Foods. 8 (5) (2019) 155, https://doi.org/10.3390/foods8050155.
[48] V.K.R. Surasani, A. Singh, A. Gupta, S. Sharma, Functionality and cooking characteristics of pasta supplemented with protein isolate from pangas processing waste, LWT Food Sci. Technol. 111 (2019) 443–448, https://doi.org/10.1016/j.lwt.2019.05.014.
[49] W. Wang, W.T. Chen, H. Yang, M. Cui, Textural and rheological properties of potato starch as affected by amino acids, Int. J. Food Prop. 20 (2018) S3123–S3134, https://doi.org/10.1080/10942912.2017.1396475.
[50] V. Marboh, C.L. Mahanta, Physicochemical and rheological properties and *in vitro* digestibility of heat moisture treated and annealed starch of sohphlang (*Flemingia vestita*) tuber, Int. J. Biol. Macromol. 168 (2021) 486–495, https://doi.org/10.1016/j.ijbiomac.2020.12.065.
[51] M. Piecyk, K. Domian, Effects of heat-moisture treatment conditions on the physicochemical properties and digestibility of field bean starch (*Vicia faba* var. minor), Int. J. Biol. Macromol. 182 (2021) 425–433, https://doi.org/10.1016/j.ijbiomac.2021.04.015.
[52] A. Sinhmar, A.K. Pathera, S. Sharma, M. Nehra, R. Thory, V. Nain, Impact of various modification methods on physicochemical and functional properties of starch: A Review, Starch-Stärke 75 (1-2) (2023) 2200117, https://doi.org/10.1002/star.202200117.
[53] Q.J. Sun, C. Xiong, Functional and pasting properties of pea starch and peanut protein isolate blends, Carbohydr. Polym. 101 (2014) 1134–1139, https://doi.org/10.1016/j.carbpol.2013.10.064.
[54] V.C. Okonkwo, E.M. Kwofie, O.I. Mba, M.O. Ngadi, Impact of thermo-sonication on quality indices of starch-based sauces, Ultrason. Sonochem. 73 (2021) 105473, https://doi.org/10.1016/j.ultsonch.2021.105473.
[55] X.J. Yang, C.D. Chi, X.L. Liu, Y.Y. Zhang, H. Zhang, H.W. Wang, Understanding the structural and digestion changes of starch in heat-moisture treated polished rice grains with varying amylose content, Int. J. Biol. Macromol. 139 (2019) 785–792, https://doi.org/10.1016/j.ijbiomac.2019.08.051.
[56] D. Le Botlan, Y. Rugraff, C. Martin, P. Colonna, Quantitative determination of bound water in wheat starch by time domain NMR spectroscopy, Carbohydr. Res. 308 (1–2) (1998) 29–36, https://doi.org/10.1016/s0008-6215(98)00068-8.
[57] V.M. Mathobo, H. Silungwe, S.E. Ramashia, T.A. Anyasi, Effects of heat-moisture treatment on the thermal, functional properties and composition of cereal, legume and tuber starches-a review, J. Food Sci. Technol. 58 (2) (2021) 412–426, https://doi.org/10.1007/s13197-020-04520-4.
[58] X. Zhao, Y. Wang, D. Li, L.J. Wang, Insight into the biphasic transition of heat-moisture treated waxy maize starch through controlled gelatinization, Food Chem. 341 (1) (2021) 128214, https://doi.org/10.1016/j.foodchem.2020.128214.
[59] C. Collar, E. Armero, Impact of heat moisture treatment and hydration level on physico-chemical and viscoelastic properties of doughs from wheat-barley composite flours, Eur. Food Res. Technol. 244 (2) (2018) 355–366, https://doi.org/10.1007/s00217-017-2961-8.